

## Solid-State Synthesis of a Conducting Polythiophene via an Unprecedented Heterocyclic Coupling Reaction

Hong Meng,<sup>†</sup> Dmitrii F. Perepichka,<sup>†,‡</sup> Michael Bendikov,<sup>†</sup> Fred Wudl,<sup>\*,†</sup>  
Grant Z. Pan,<sup>§</sup> Wenjiang Yu,<sup>‡</sup> Wenjian Dong,<sup>‡</sup> and Stuart Brown<sup>‡</sup>

Contribution from the Department of Chemistry and Biochemistry and the Exotic Materials Institute, Microfabrication Lab, Department of Physics and Astrophysics, University of California, Los Angeles, California 90095-1569, and INRS-Énergie, Matériaux et Télécommunications, Université du Québec, Varennes, Québec J3X 1S2, Canada

Received July 7, 2003; E-mail: wudl@chem.ucla.edu

**Abstract:** Prolonged storage (~2 years) or gentle heating (50–80 °C) of crystalline 2,5-dibromo-3,4-ethylenedioxythiophene (DBEDOT) affords a highly conducting, bromine-doped poly(3,4-ethylenedioxythiophene) (PEDOT), as confirmed by solid-state NMR, FTIR, CV, and vis–NIR spectroscopies. The novel solid-state polymerization (SSP) does not occur for 2,5-dichloro-3,4-ethylenedioxythiophene (DCEDOT), and requires a much higher temperature (>130 °C) for 2,5-diiodo-3,4-ethylenedioxythiophene (DIEDOT). X-ray structural analysis of the above dihalothiophenes reveals short Hal···Hal distances between adjacent molecules in DBEDOT and DIEDOT, but not in DCEDOT. The polymerization may also occur in the melt but is significantly slower and leads to poorly conductive material. Detailed studies of the reaction were performed using ESR, DSC, microscopy, and gravimetric analyses. SSP starts on crystal defect sites; it is exothermic by 14 kcal/mol and requires activation energy of ~26 kcal/mol (for DBEDOT). The temperature dependence of the conductivity of SSP-PEDOT ( $\sigma_{\text{r}} = 20\text{--}80$  S/cm) reveals a slight thermal activation. It can be further increased by a factor of 2 by doping with iodine. Using this approach, thin films of PEDOT with conductivity as high as 20 S/cm were fabricated on insulating flexible plastic surfaces.

### Introduction

Of all the polythiophenes which have received much attention in recent years for their unique electrical properties,<sup>1,2</sup> one of the most studied is poly(3,4-ethylenedioxythiophene) (PEDOT).<sup>3</sup> Owing to its excellent electronic properties (electrical conductivity, electrochromic properties, etc.) and high stability, PEDOT is one of the most industrially important conjugated polymers. PEDOT was first synthesized in the early 1990s and was initially commercialized in antistatic coatings.<sup>3b</sup> Due to a stereoregularity of the only possible polymer structure, it has a very high conductivity (up to 550 S/cm in the electrochemical doped state).<sup>3</sup> The remarkable stability of PEDOT in its doped state, compared with other conducting polymers, allows a number of potential applications.<sup>3</sup>

While traditional oxidative polymerization with  $\text{FeCl}_3$  in organic solvents gives an insoluble blue-black doped polymer powder,<sup>3d</sup> the use of a water-soluble electrolyte [polystyrene sulfonic acid (PSS)] as a charge-balancing dopant during polymerization, affords a processable polymer solution (commercial product, Baytron) that forms semitransparent conducting films<sup>4</sup> upon spin-casting. To obtain the neutral polymer, a nickel (0) complex-promoted polycondensation of 2,5-dihalo-3,4-ethylenedioxythiophenes has been employed.<sup>5</sup> However, these attempts gave either nonprocessable PEDOT<sup>5a,d</sup> or polydisperse oligomeric material.<sup>5b,c</sup> Consequently, the limitations of traditional polymerization methods can be a serious problem for PEDOT applications as well as for in-depth investigation of molecular order in this conducting polymer.<sup>6</sup> It is generally not possible to obtain a well-defined polymer structure, unless the synthesis of conducting polymers is carried out via pure chemical polymerization routes, without adding any catalysts. A possible solution for this lies in a solid-state polymerization of a structurally pre-organized crystalline monomer.

<sup>†</sup> Exotic Materials Institute and Department of Chemistry and Biochemistry, University of California.

<sup>§</sup> Microfabrication Lab, University of California.

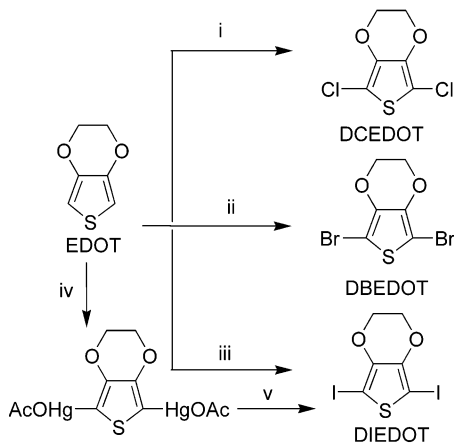
<sup>‡</sup> Department of Physics and Astrophysics, University of California.

<sup>‡</sup> INRS-Énergie, Matériaux et Télécommunications, Université du Québec.

- (1) (a) Roncali, J. *Chem. Rev.* **1992**, *92*, 711. (b) *Handbook of Oligo- and Polythiophenes*; Fichou, D., Ed.; Wiley-VCH: Weinheim, Germany, 1999. (c) *Handbook of Conducting Polymers*, 2nd ed.; Skotheim, T. A., Elsenbaumer, R. L., Reynolds, J. R., Eds.; Marcel Dekker: New York, 1998.
- (2) *Handbook of Organic Conductive Molecules and Polymers*; Nalwa, H. S., Ed.; John Wiley & Sons: New York, 1997; Vol. 2.
- (3) (a) Groenendaal, L. B.; Jonas, F.; Freitag, D.; Pielartzik, H.; Reynolds, J. R. *Adv. Mater.* **2000**, *12*, 481. (b) Jonas, F.; Heywang, G.; Gladbach, B.; Schmidtberg, W.; Heinze, J.; Dietrich, M. U.S. Patent No. 5,035,926, 1991. (c) Groenendaal, L. B.; Zotti, G.; Aubert, P.-H.; Waybright, S. M.; Reynolds, J. R. *Adv. Mater.* **2003**, *115*, 855. (d) Jonas, F.; Schrader, L. *Synth. Met.* **1991**, *41–43*, 831.

- (4) Zhang, F.; Johansson, M.; Andersson, M. R.; Hummelen, J. C.; Inganäs, O. *Adv. Mater.* **2002**, *14*, 662.

- (5) (a) Yamamoto, T.; Abla, M. *Synth. Met.* **1999**, *100*, 237. (b) Tran-Van, F.; Garreau, S.; Louarn, G.; Froyer, G.; Chevrot, C. *Synth. Met.* **2001**, *119*, 381. (c) Tran-Van, F.; Garreau, S.; Louarn, G.; Froyer, G.; Chevrot, C. *J. Mater. Chem.* **2001**, *11*, 1378. (d) Yamamoto, T.; Shiraiishi, K.; Abla, M.; Yamaguchi, I.; Groenendaal, L. B. *Polymer* **2002**, *43*, 711.
- (6) (a) Mo, Z.; Lee, K.-B.; Moon, Y. B.; Kobayashi, M.; Heeger, A. J.; Wudl, F. *Macromolecules* **1985**, *18*, 1972. (b) Fichou, D. *J. Mater. Chem.* **2000**, *10*, 571. (c) Aasmundtveit, K. E.; Samuelsen, E. J.; Pettersson, L. A. A.; Inganäs, O.; Johansson, T.; Feidenhans, R. *Synth. Met.* **1999**, *101*, 561.

**Scheme 1.** Synthesis of Dihalo-EDOT Monomers<sup>a</sup>

<sup>a</sup> Reagents and conditions: (i) *N*-chlorosuccinimide,  $\text{CHCl}_3/\text{AcOH}$ , 5 °C, 8 h; (ii) *N*-bromosuccinimide,  $\text{CHCl}_3/\text{AcOH}$ , 5 °C, 8 h; (iii) 1) BuLi, THF,  $-78\text{ °C} \rightarrow 0\text{ °C}$ , 1 h, 2)  $\text{I}_2$ ,  $-78\text{ °C} \rightarrow 0\text{ °C}$ , 12 h; (iv)  $\text{Hg}(\text{OAc})_2$ , AcOH, 20 °C, 12 h; (v)  $\text{I}_2$ , MeCN, 20 °C, 2 h.

The idea of solid-state polymerization of a suitable monomer in a well-ordered crystalline state was realized in the 1960s and 1970s with polydiacetylenes<sup>7,8</sup> and  $(\text{SN})_x$ .<sup>9</sup> However, until this year,<sup>10,11</sup> there were no reports regarding the solid-state synthesis of the most widely investigated conducting polymers—the polythiophenes. The importance of this goal is emphasized by the high potential of polythiophenes for industrial applications, as compared to other conducting polymers.<sup>2</sup> For example, the synthesis of PEDOT is still confined to chemical or electrochemical oxidation of monomer solutions.<sup>3</sup>

We have recently reported a facile solid-state polymerization of 2,5-dibromo-3,4-ethylenedioxythiophene (DBEDOT) to give PEDOT through an unprecedented catalyst-free cross-coupling reaction.<sup>10</sup> This discovery has already found resonance in the research community.<sup>11</sup> In this contribution, we describe the X-ray structure of the dihalothiophenes, detailed studies of the mechanism of their solid-state polymerization and characterization of the polymer.

## Results and Discussions

**Synthesis.** Dihalogen-substituted derivatives of 3,4-ethylenedioxythiophene (EDOT), 2,5-dibromo-3,4-ethylenedioxythiophene (DBEDOT)<sup>12</sup> and 2,5-dichloro-3,4-ethylenedioxythiophene (DCEDOT)<sup>5d</sup> have been prepared by direct halogenation of EDOT according to known procedures (Scheme 1). 2,5-Diiodo-3,4-ethylenedioxythiophene (DIEDOT) was synthesized by iodination of either dilithium-EDOT or bis(acetoxymercury)-EDOT with molecular iodine. The EDOT derivatives are colorless crystalline materials which can be almost quantitatively

**Table 1.** Elemental Analysis of PEDOT Samples Prepared in Different Conditions

sample <sup>a</sup>	C, %	H, %	S, %	Hal, %	calculated formula
PEDOT-A	28.87	1.65	12.90	38.42	$\text{C}_{6.0}\text{H}_{4.10}\text{S}_{1.0}\text{Br}_{1.2}$
PEDOT-B	36.74	2.18	16.33	12.57	$\text{C}_{6.0}\text{H}_{4.3}\text{S}_{0.99}\text{Br}_{0.31}$
PEDOT-C	46.84	2.42	19.04	0.42	$\text{C}_{6.0}\text{H}_{3.7}\text{S}_{0.91}\text{Br}_{0.08}$
PEDOT-D <sup>b</sup>	46.11	2.85	16.85	4.96	$\text{C}_{6.0}\text{H}_{4.4}\text{S}_{0.82}\text{Cl}_{0.22}\text{Fe}_{0.02}$
PEDOT-E	22.26	1.18	9.62	55.95	$\text{C}_{6.0}\text{H}_{3.8}\text{S}_{0.97}\text{I}_{1.43}$

<sup>a</sup> Polymerization conditions. A: DBEDOT crystals heated at 60 °C for 1 day under Ar, after vacuum-drying at 20 °C overnight; B: DBEDOT stored for two years, after vacuum-drying at 20 °C overnight; C: PEDOT-B after dedoping with  $\text{NH}_2\text{NH}_2 \cdot \text{H}_2\text{O}$ ; D:  $\text{FeCl}_3$  synthesized PEDOT after dedoping with  $\text{NH}_2\text{NH}_2 \cdot \text{H}_2\text{O}$ ; E: DIEDOT crystals heated at 140 °C for 3 days, after vacuum-drying at 70 °C overnight <sup>b</sup> 0.80% of Fe was also found in this sample.

sublimed by gentle heating in a vacuum (or even at normal pressure in a nitrogen flow, for small quantities). X-ray-quality single crystals of DBEDOT, DCEDOT, and DIEDOT were obtained by slow evaporation of ethanol solutions or sublimation.

The polymerization of DBEDOT was discovered by chance as a result of prolonged storage (2 years) of the monomer at room temperature.<sup>10</sup> The colorless crystalline DBEDOT, with time, transformed into a black material without apparent change of morphology. Surprisingly, the conductivity of this decomposition product appeared to be very high (up to 80 S/cm) for an organic solid. Even though this type of noncatalytic coupling was not known in organic chemistry, indeed, the most likely explanation for the observed transformation was polymerization with formation of bromine-doped PEDOT. The following characterizations unequivocally confirmed the proposed structure (see below).

The reaction was not affected by air, vacuum, or light and was even successful in hot water. When the reaction occurred in a closed vial, release of a significant amount of elemental bromine was detected. Increasing the temperature up to the melting point (97 °C) significantly decreased the reaction time; however, the material's solid state is an essential prerequisite: quick heating above the melting point resulted in a nondecomposing very slowly polymerizing melt of DBEDOT [see Supporting Information (SI)]. Likewise, no polymerization was observed in solutions, even at moderately high temperatures (>100 °C).

**Characterization of the Polymerization Product.** The polymer is a black solid (blue in thin films), insoluble in organic solvents. Thermogravimetric analysis of a dedoped sample indicated that it was stable up to 330 °C (<10% weight loss). The same analysis of an “as prepared” sample showed that weight loss started already slightly above rt, due to loss of molecular bromine ( $\text{Br}_3^- \rightarrow \text{Br}^- + \text{Br}_2$ , see below). An  $\text{FeCl}_3$ -synthesized PEDOT sample was stable up to 280 °C (10% of weight lost, see SI). Dissolution in strong acids (e.g., sulfuric or trifluorosulfonic acid, but not trifluoroacetic acid) gives a deep-blue solution and releases molecular bromine. Subsequent dilution with water allows recovery of dark-blue PEDOT powder, which is ca. one-half as conductive as pristine, solid-state polymerized PEDOT (SSP-PEDOT). The sample of  $\text{FeCl}_3$ -synthesized PEDOT showed the same behavior.

**Molecular Composition of the Polymer.** Elemental analysis indicates that the “as prepared” vacuum-dried SSP-PEDOT (sample PEDOT-A) is heavily doped with bromine (Table 1).

- (7) (a) Magat, M. *Polymer* **1962**, *3*, 449. (b) Baughman, R. H. *J. Polym. Sci.: Polym. Phys. Ed.* **1974**, *12*, 1511.  
 (8) (a) Wegner, G. *Z. Naturforsch.* **1969**, *24b*, 824. (b) Wegner, G. *Makromol. Chem.* **1971**, *145*, 85. (c) Enkelmann, V.; Schleier, G.; Wegner, G. *Chem. Phys. Lett.* **1977**, *52*, 314. (d) Yee, K. C.; Chance, R. R. *J. Polym. Sci.: Polym. Phys. Ed.* **1978**, *16*, 431.  
 (9) (a) Walatka, V. V., Jr.; Labes, M. M.; Perlstein, J. H. *Phys. Rev. Lett.* **1973**, *31*, 1139. (b) Cohen, M. J.; Garito, A. F.; Heeger, A. J.; MacDiarmid, A. G.; Mikulski, C. M.; Saran, M. S.; Kleppinger, J. *J. Am. Chem. Soc.* **1976**, *98*, 3844.  
 (10) Meng, H.; Perepichka, D. F.; Wudl, F. *Angew. Chem., Int. Ed.* **2003**, *42*, 658.  
 (11) Spencer, H. J.; Berridge, R.; Crouch, D. J.; Wright, S. P.; Giles, M.; McCulloch, I.; Coles, S. J.; Hursthouse, M. B.; Skabara, P. J. *J. Mater. Chem.* **2003**, *13*, 2075.  
 (12) Sotzing, G. A.; Reynolds, J. R.; Steel, P. J. *Chem. Mater.* **1996**, *8*, 882.

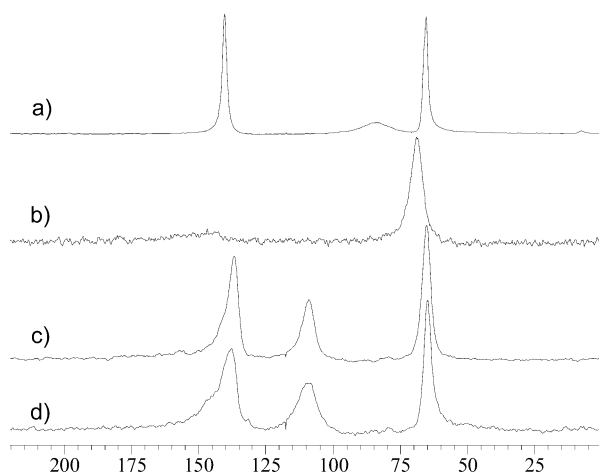


**Figure 1.** Solid-state CP-MAS  $^{13}\text{C}$  NMR spectra of (a) DBEDOT monomer and polymer PEDOT (b) as prepared by SSP, (c) SSP, after dedoping, (d) prepared by  $\text{FeCl}_3$  oxidation, after dedoping.

The composition of the polymer has a correct ratio of C, H, S (6:4:1) and contains 1.2 atoms of bromine per each EDOT unit. This reflects the maximum possible doping level (two  $\text{Br}_3^-$  anions and, therefore, a bipolaron per every five thiophene units) of polythiophene.<sup>13</sup> After dedoping with hydrazine in acetonitrile solution, the polymer still had a trace amount of bromine (0.42%), possibly due to the unreacted C–Br end groups on the polymer chain. Assuming the residual bromine in the elemental analysis is due to covalently bound bromine end groups of the PEDOT chain that are not expected to be displaced with hydrazine at room temperature, the low amount of bromine suggests an average molecular weight of the polymer of  $>30$  kDa (i.e. ca.  $>200$  thiophene units in the chain). Interestingly, a room-temperature synthesized, 2 year-old sample (PEDOT-B), has significantly lower bromine content, when compared to a PEDOT-A sample synthesized at  $60^\circ\text{C}$ . This suggests that the observed high doping level is due to bromine kinetically trapped in the crystal cage, rather than a thermodynamically stable state.

Laser desorption ionization mass-spectral analysis of a PEDOT-A crystalline sample shows a weak signal at  $m/z$  1821, corresponding to a  $[(\text{EDOT})_{13}\text{H}]^+$  fragment and an increasing-intensity sequence of lower-molecular weight fragments differing by one EDOT unit (MW = 140):  $m/z$  1681, 1541, etc. Although we could not detect higher-molecular weight ions (which are less volatile under MS conditions), the actual molecular weight of the polymer should be higher than 1820, as the polymer molecule should be end-capped with bromine atoms, not found in the heaviest detected ion.

**NMR Spectroscopy.** Solid-state CP-MAS  $^{13}\text{C}$  NMR spectroscopic studies were performed to establish the structure of the polymer. The spectrum of the starting DBEDOT (Figure 1a) changes drastically during the polymerization (Figure 1b). Owing to the radical character of polarons in doped polythiophene (see below), the NMR signals suffer a strong paramagnetic broadening which, as expected, was very strong for the thiophene nuclei atoms and less so for the remote oxyethylene bridge. Dedoping with hydrazine destroys the radical character of the polymer, and higher resolution of the spectrum is restored (Figure 1c). The peak at  $\delta$  65 ppm is

(13) Patil, A. O.; Heeger, A. J.; Wudl, F. *Chem. Rev.* **1988**, *88*, 183.

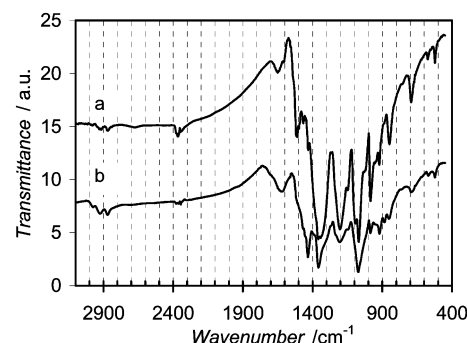


**Figure 2.** FT-IR spectra of the dedoped PEDOT prepared by (a) solid-state polymerization and (b)  $\text{FeCl}_3$  oxidation polymerization in solution (KBr pellets).

unequivocally assigned to the aliphatic carbons ( $\text{OCH}_2$ ), and its position does not change during the polymerization. The signal due to the 2,5-C atoms of the thiophene ring shifts significantly, from  $\delta$  84 to 108 ppm, following the substitution of bromine atoms in DBEDOT with carbon in PEDOT. The signal due to the 3,4-C atoms undergoes only a small change, from  $\delta$  140 to 138 ppm. Both SSP and  $\text{FeCl}_3$ -synthesized polymers show practically identical signals, indicating essentially the same chemical structure. The half-widths of the 2,5-C and 3,4-C peaks in  $\text{FeCl}_3$ -PEDOT are twice as large as that of SSP-PEDOT, which might be a result of a lower polydispersity in the latter.

**FTIR Spectroscopy.** As in the case of NMR spectroscopy, the FTIR analysis of the as-prepared, doped polymer is hindered by strong electronic absorption (see below) in the IR region. FTIR comparative analysis of SSP- and  $\text{FeCl}_3$ -PEDOT dedoped samples revealed very similar spectra for both samples, showing weak characteristic  $\text{CH}_2$  stretchings of the dioxyethylene bridge ( $2850\text{--}3000\text{ cm}^{-1}$ ) and very strong C–O ( $1200$  and  $1070\text{ cm}^{-1}$ ) and C=C characteristic bands ( $1357\text{ cm}^{-1}$ ) (Figure 2).

**UV–Vis–NIR Spectroscopy.** The electronic spectrum of an SSP-PEDOT thin film prepared by in situ sublimation/polymerization of DBEDOT (see “Applications in Plastic Electronics”) is very similar to that previously reported for fully doped PEDOT:<sup>14</sup> the only absorption in the vis–NIR region<sup>15</sup> is a very broad band, starting at ca. 500 nm and extending into the mid-IR region (beyond 3000 nm; a tail of this band is seen in FTIR spectra) (Figure 3). Dedoping with hydrazine results in immediate change of the film from sky blue to dark violet. In situ spectral monitoring of the dedoping process shows a very fast reduction of the near-IR band, characteristic of a bipolaron state of PEDOT and emergence of a new band at  $\lambda_{\text{max}} \approx 550$  nm, due to the neutral state. A band gap of 1.63 eV can be estimated from the red-edge of this band ( $\sim 760$  nm). A shoulder at  $\sim 900$  nm and a NIR band at  $\sim 2000$  nm are due to intermediate formation of a polaron (radical cation) state, and the intensity of these bands drops quite slowly with time (a trace of these bands is seen even after 2 h of soaking the film in hydrazine solution). Difficulties in complete dedoping of PEDOT films can be explained by the strong electron-donor character of neutral PEDOT, allowing air-doping; indeed, when the dedoped

(14) Dietrich, M.; Heinze, J.; Heywang, G.; Jonas, F. J. *Electroanal. Chem.* **1994**, *369*, 87. (b) Ahonen, H. J.; Lukkari, J.; Kankare, J. *Macromolecules* **2000**, *33*, 6787.

(15) There is also a UV absorption at ca. 300 nm, not observed in electrochemically doped PEDOT and attributed to absorbance of  $\text{Br}_3^-$  counterion.



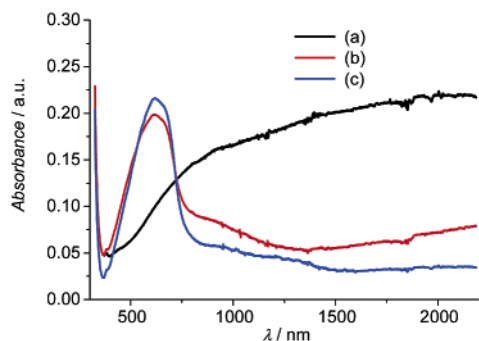


**Figure 3.** UV-vis-NIR spectra of the SSP-PEDOT film on glass slide substrate (a) “as formed”, (b) after dedoping in hydrazine solution for 5 min, (c) after dedoping during 50 min.

**Table 2.** Conductivity Data of the PEDOT Polymer Measured at Room Temperature<sup>a</sup>

reaction temperature (°C) reaction time	$\sigma_n$ (SSP-PEDOT)/ S cm <sup>-1</sup>				$\sigma_n$ (FeCl <sub>3</sub> -PEDOT)/ S cm <sup>-1</sup>
	20 2 years <sup>b</sup>	60 24 h	80 4 h	120 24 h	0–5 24 h
“crystals”/“fibers”	80	33	20	NA	NA
pellets as synthesized	30	18	16	0.1	NA
pellets after I <sub>2</sub> doping	53	30	27	5.8	7.6
thin films	NA	23	NA	NA	NA
thin films after I <sub>2</sub> doping	NA	48	NA	NA	NA

<sup>a</sup> Reported values are an average of at least three measurements (reproducibility of each measurement is  $\pm 30\%$ ). <sup>b</sup> The monomer was stored in a closed jar for 2 years at room temperature (ca. 20 °C).

film was removed from hydrazine solution and rinsed, a slow increase in the intensity of the radical-cation bands was observed.

**Electrochemistry.** A cyclic voltammetry experiment was performed on a thin polymer film deposited by in situ sublimation/polymerization on a platinum electrode. On anodic sweeping, SSP-PEDOT exhibits a quasi-reversible oxidation wave at  $E^{p.a.ox} = 0.07$  V vs Ag/Ag<sup>+</sup>, resulting in *p*-doping of the polymer (see SI). On reverse scan, a cathodic peak is seen at considerably more negative potential ( $E^{p.c.ox} = -0.62$  V). Multiple scanning between  $-1$  and  $+0.2$  V reveals high stability of the material: less than 1% reduction of the current was observed after 50 repetitive scans. Scanning into more negative potentials results in an irreversible reduction wave at  $E^{p.c.red} = -2.15$  V vs Ag/Ag<sup>+</sup>. The band gap  $E_g = 1.65$  eV was determined from the onset of the *n*- and *p*-doping waves. These values are comparable with those of electrochemically polymerized PEDOT films.<sup>14</sup>

**Electrical Conductivity.** The room-temperature conductivity of different SSP-PEDOT samples was measured by the four-probe method (Table 2). The highest conductivity belongs to the polymer prepared at lowest temperature and longest reaction time (PEDOT-B, Table 1), which may reflect achievement of a higher degree of order. Indeed, heating above the monomer’s melting point results in dramatically reduced conductivity (0.1 S/cm), which rises up to 5.8 S/cm after doping with iodine, approaching the value of an FeCl<sub>3</sub>-synthesized PEDOT (7.6 S/cm). Not very significant, but certain increase in conductivity of SSP-PEDOT (ca. 2 times) was found on exposing a sample to iodine vapor. The temperature dependence of the conductivity (Figure 4) reveals a typical semiconductive behavior, and no semiconductor–metal transition was found down to 20 K. This behavior is in contrast to the previously observed behavior of

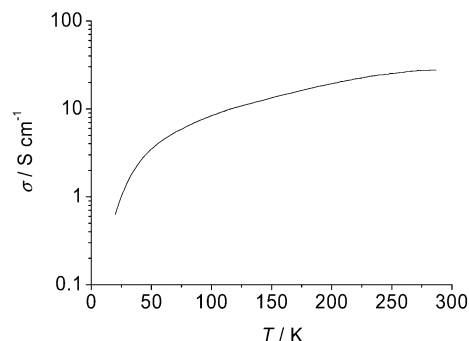


**Figure 4.** Four-probe measurement of the temperature dependence of conductivity of SSP-PEDOT.

“metallic” PEDOT materials, electrochemically doped with PF<sub>6</sub><sup>-</sup>, BF<sub>4</sub><sup>-</sup>, and ClO<sub>4</sub><sup>-</sup>.<sup>16</sup>

**ESR Spectroscopy.** Like most other conductive polymers such as polypyrrole and polyacetylene, the conductivity of the doped SSP-PEDOT is brought about by dication and radical cation charge carriers.<sup>17</sup> Consequently, a strong ESR signal was observed at  $g \approx 2.004$ , with a temperature- and doping level-dependent shape. When the temperature increased from 5 to 300 K, the ESR signal line-shape changed from a symmetric narrow line (line width ca. 5 G) to a broad line (20 G) with the right wing much broader than the left (Figure 5a). Similar behavior was observed in other conducting polymers and is indicative of increased conductivity with increasing temperature.<sup>2</sup> The ESR line width is determined by the relaxation rate of the radical and is a characteristic of the degree of delocalization. Therefore, the increase in line width with temperature is in agreement with the temperature dependence of conductivity (Figure 4). Interestingly, the temperature dependence of the ESR signal integrated intensity ( $I_{ESR}$ ) follows the Curie law ( $\chi_c \approx I_{ESR} = C/T$ ): a perfectly straight line crosses the (0,0) point (Figure 5b), which is characteristic of standard paramagnetic behavior with no (anti)ferromagnetic ordering. This trend is not usual for highly conducting media and is in contrast to previous observations in other conducting polymers, including electropolymerized PEDOT, where a strong contribution from Pauli-type spin susceptibility (temperature-independent) was observed.<sup>16,18,19</sup>

**Microscopic Analysis.** At small magnification ( $\times 100$ ), there is no visible change in morphology on polymerization: the colorless needle-shaped crystals of DBEDOT gradually transform into black crystals (Figure 6a). However, on higher magnification, it is seen that the crystal surface is damaged during polymerization (Figure 6b). The anisotropic character of the defects can be clearly seen on the “crystal” cut, Figure 6c,d, where a layered structure might reflect some order in the formation of a polymer chain.

**Wide-Angle XRD Analysis.** To shed light on the question of possible crystalline order, we performed wide-angle X-ray powder diffraction (XRD) studies on SSP-PEDOT (2-year old sample PEDOT-B, Figure 7a) and in thin film form (polymerized for 24 h at 60 °C, Figure 7b). Even though both samples

(16) Kieboom, R.; Aleshin, A.; Hutchison, K.; Wudl, F.; Heeger, A. J. *Synth. Met.* **1999**, *101*, 436.

(17) (a) Pereira, E. C.; Bulhoões, L. O. S.; Pawlicka, A.; Nascimento, O. R.; Faria, R. M.; Walmsley, L. *Phys. Rev. B* **1994**, *50*, 3648. (b) Demirboğa, B.; Onal, A. M. *J. Phys. Chem. Solids* **2000**, *61*, 907.

(18) (a) Mizoguchi, K. *Synth. Met.* **2001**, *119*, 35. (b) Eichele, H.; Schwoerer, M.; Huber, R.; Bloor, D. *Chem. Phys. Lett.* **1976**, *42*, 342.

(19) This comparison should be made with reservation, since our experiments measured spin-susceptibility only and not total susceptibility.

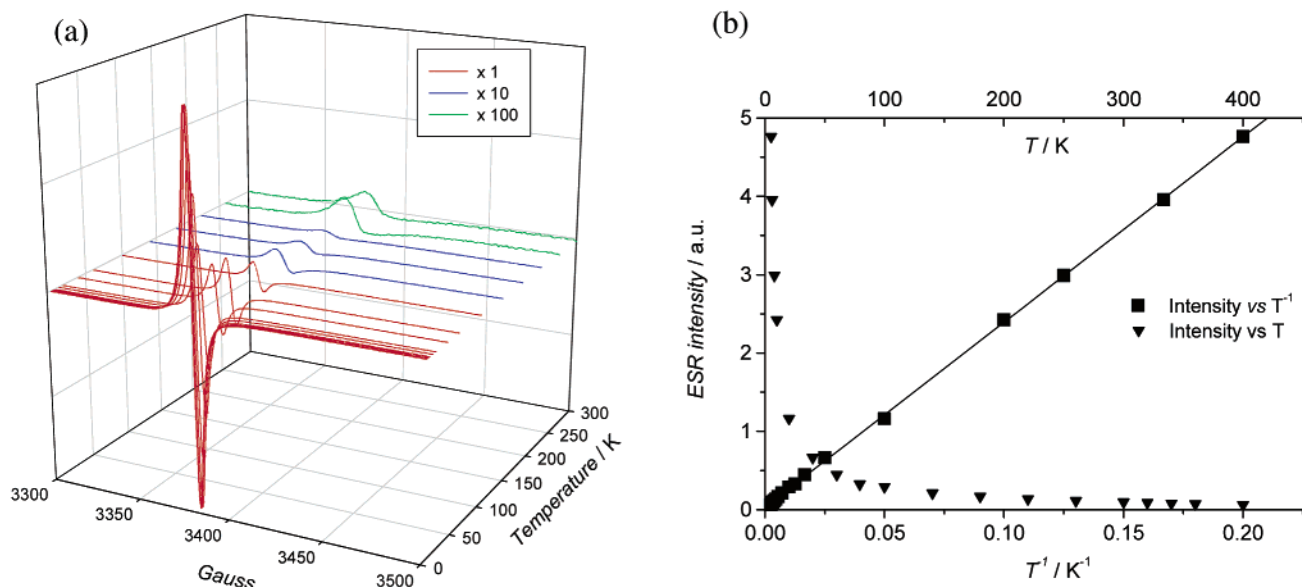


**Figure 5.** Temperature dependence of the ESR spectrum of SSP-PEDOT. (a) Evolution of the ESR signal (5–300 K interval); (b) temperature dependence of the ESR integrated signal intensity (5–400 K interval).

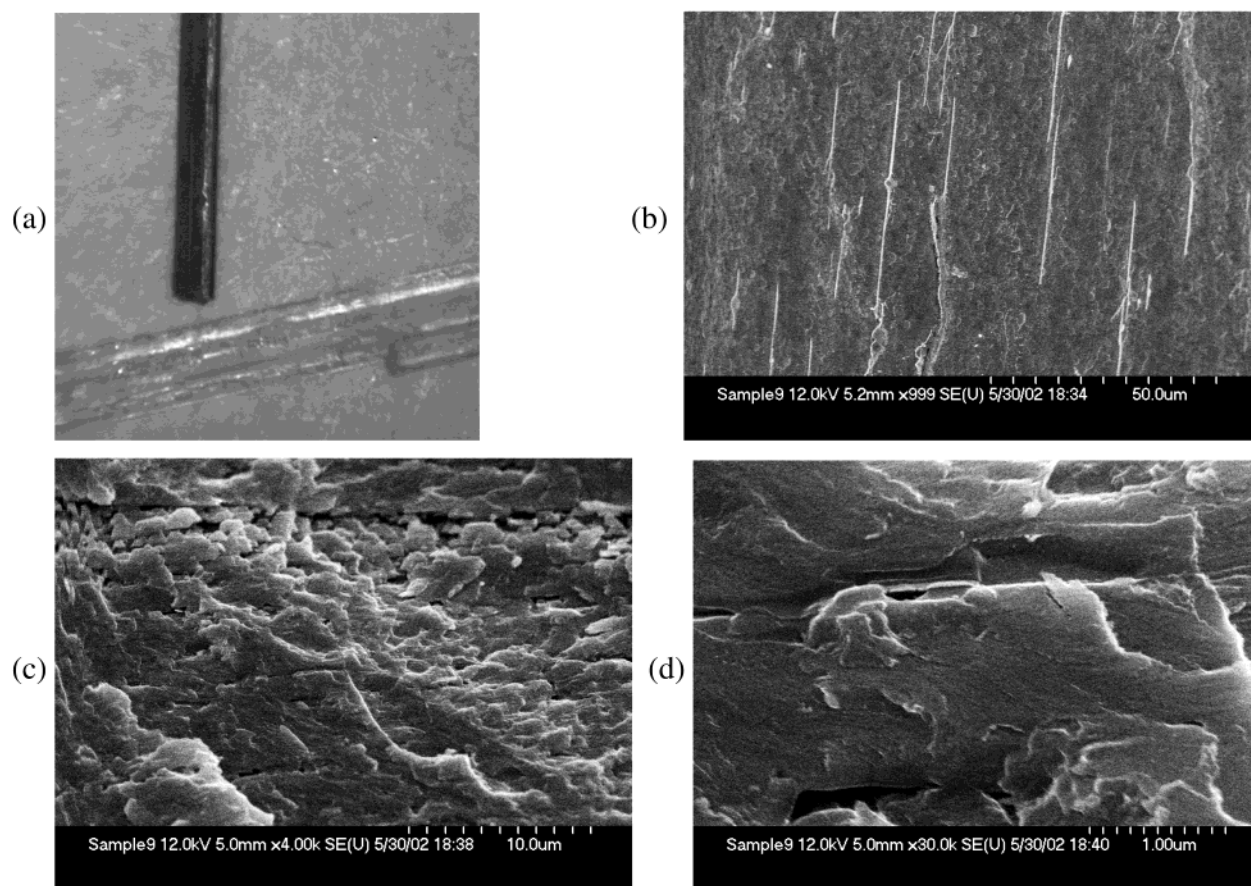


**Figure 6.** (a) Preservation of the crystal morphology of DBEDOT (colorless crystal, bottom) upon conversion to PEDOT (black crystal, top), optical microscopy image; (b) surface of SSP-PEDOT “crystal” under higher SEM magnification; (c) and (d) enlargement of a cut of an SSP-PEDOT crystal, showing layered structure.

are significantly disordered, compared to the crystalline DBEDOT (Figure 7c), strong and quite sharp (line width ca.  $0.3^\circ$ ) diffraction peaks observed at  $2\theta = 29.4, 36.0, 39.5, 43.2, 47.7, 48.6^\circ$  reveal relatively long-range order. A stronger signal was observed for the thin film sample. These peaks obviously do not belong to the starting DBEDOT, which is characterized by

main peaks at  $2\theta = 8.6, 17.0, 25.4, 27.0, 29.1, \text{ and } 34.0^\circ$ , and thus must be attributed to the structure of the formed polymer. The strongest peak in the DBEDOT diffractogram corresponds to a  $d$  spacing of  $3.50 \text{ \AA}$ , which is an interplane distance between the DBEDOT molecules in the stack (see Crystallographic section). A close (but different) reflection at  $26.0^\circ$  corresponding

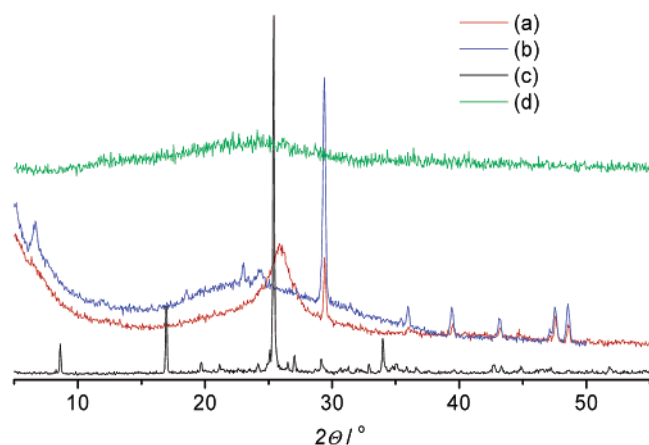


**Figure 7.** XRD spectra of (a) PEDOT-B sample (see Table 1), (b) SSP-PEDOT thin film deposited on glass substrate, (c) DBEDOT monomer, and (d) FeCl<sub>3</sub>-synthesized PEDOT.

to a lower  $d$  spacing of 3.42 Å was observed in the PEDOT-B powder sample (Figure 7, line a) as a very broad peak (line width  $\sim 3^\circ$ ). This reflection at  $26^\circ$  has been occasionally observed in several samples as a narrower peak and should probably be attributed to a different phase. It is possible that excess bromine, which is kinetically trapped in the SSP-PEDOT crystal lattice (especially, in thick crystals), is the most significant contributor to the amorphous part of the XRD spectra. Not surprisingly, these sharp peaks were not observed in the PEDOT powder or thin films samples, obtained by solution polymerization techniques.<sup>5d,6c</sup> Furthermore, the control XRD measurement of FeCl<sub>3</sub>-synthesized PEDOT indicated an amorphous solid. However, it was reported that polythiophene with some degree of crystallinity can be achieved by high-temperature annealing,<sup>6a,c</sup> and by electrochemical polymerization under precise potential control.<sup>20</sup>

**Reaction Mechanism Studies.** Thermomicroscopy monitoring of the polymerization process with slow-time regime movie recording was undertaken to understand the macroscopic features of the reaction (see SI). When the DBEDOT crystals were heated at  $92^\circ\text{C}$  (i.e., below the melting point), a polymerization process, observed as a darkening of the crystal, took place after a ca. 20-min induction period. Importantly, the color change was not uniform throughout the crystal, but occurred as a polymerization “wave” initiated from several points, which indicates that the crystal defects act as intuitively expected reaction centers. The SSP process does not appear to be dependent on the sample morphology, size, or purification method. Indeed, rigorous purification of DBEDOT by column chromatography, several recrystallizations, and vacuum sublimation has no apparent effect on the reaction rate (although accelerated polymerization was indeed observed for a crude, unpurified sample). The liquid-state behavior of the DBEDOT is very different: when the temperature ramp was set to  $100^\circ\text{C}$  (to rapidly melt the sample), no polymerization occurred: even heating to  $200^\circ\text{C}$  (for small samples of DBEDOT) only results in “refluxing” without any observable polymerization. However, when larger samples of the material were heated at a rate of ca.  $10^\circ\text{C}/\text{min}$ , a spontaneous polymerization was reproducibly observed at  $\sim 140^\circ\text{C}$  (see SI). We explain this by

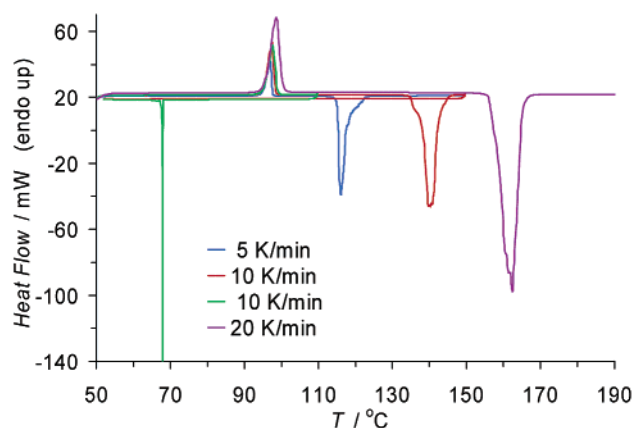


**Figure 8.** DSC curves of the DBEDOT at different heating scans. Green line shows the experiment where the temperature scan was reversed immediately after melting.

accumulation of catalytic impurities (presumably, bromine) during the heating of large samples of DBEDOT. Similar autocatalytic decomposition of liquid 2,5-dibromopyrrole can be inhibited by addition of base (tertiary amines).<sup>21</sup>

To understand the mechanism of this unique reaction, its kinetics were studied by calorimetric, gravimetric, and ESR spectroscopic methods.

**Differential Scanning Calorimetry (DSC) Studies.** Heating the monomer DBEDOT at  $5\text{--}20^\circ\text{C}/\text{min}$  results in an endothermic melting process ( $\Delta H = 4.8 \pm 0.1$  kcal/mol) before the exothermic polymerization event occurs (Figure 8). As expected, the position of the melting peak ( $95\text{--}98^\circ\text{C}$ ) is only scarcely affected by the heating rate, and when the temperature scan was reversed immediately after the melting, a very sharp exothermic crystallization peak was observed around  $65\text{--}70^\circ\text{C}$  (at a scan rate of  $10^\circ\text{C}/\text{min}$ ).

Continuing heating above the melting point results in an exothermic polymerization peak, releasing  $20 \pm 0.8$  kcal/mol, and its position changes significantly with the scan rate (Figure 8). This energy is a complex value, including polymer formation, doping, and endothermic crystallization process, which corresponds to formation of a solid polymer from the liquid DBEDOT phase (see below).

The kinetics of the SS polymerization was studied by isothermal DSC measurements. Figure 9 shows the DSC behavior of the DBEDOT monomer crystals heated at  $65\text{--}90^\circ\text{C}$  (i.e., below the melting point). The DSC curves are characterized by relatively symmetric exothermic peaks due to the polymerization reaction. The relative heat flow  $\Delta W = W - W_0$  (where  $W$  and  $W_0$  are the observed and a baseline heat flow) reflects the reaction rate ( $w = \Delta W/\nu\Delta H_p$ , where  $w$  is the reaction rate and  $\nu$  is the amount of sample in moles).<sup>22</sup> Broader peaks at low temperatures correspond to lower maximum reaction rate ( $w_{\text{max}}$ ) and, correspondingly, longer reaction time. The integration of the peaks gives the heat of polymerization,  $\Delta H_p = -14.0 \pm 1.3$  kcal/mol, which is less than the energy for liquid-phase reaction ( $-20 \pm 0.8$  kcal/mol) almost exactly by the melting enthalpy ( $4.8 \pm 0.1$  kcal/mol); i.e., the total energy of the liquid-phase polymerization and SSP is virtually the same. The conversion half-time ( $t_{1/2}$ ) was taken as a point of release of

(20) Niu, L.; Kvarnström, C.; Fröberg, K.; Ivaska, A. *Synth. Met.* **2001**, *122*, 425.

(21) Gilow, H. M.; Burton, D. E. *J. Org. Chem.* **1981**, *46*, 2221.

(22) Chance, R. R.; Patel, G. N.; Turi, E. A.; Khanna, Y. P. *J. Am. Chem. Soc.* **1976**, *100*, 1307.



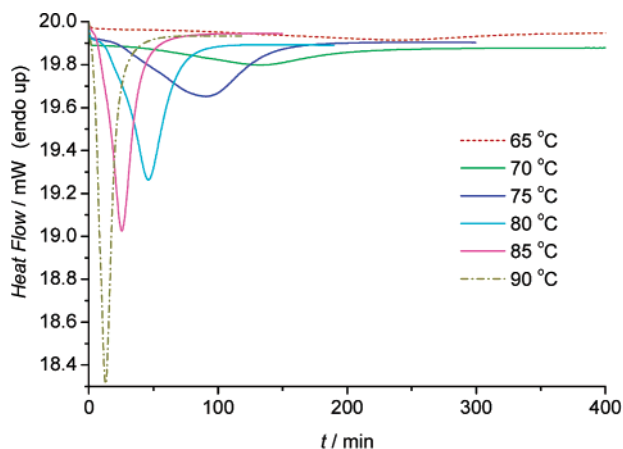


**Figure 9.** Isothermal DSC curves of the monomer crystals heated at different temperatures.

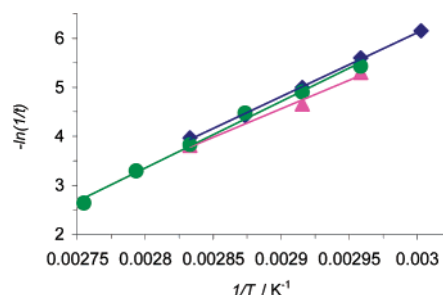


**Figure 10.** Arrhenius dependence of the SSP reaction as determined by (a) DSC (●),  $t = t_{1/2} \approx t_{\max}$ ; (b) gravimetry (▲),  $t = t_{1/2}$ ; (c) ESR (◆),  $t = t_{\max}$ .

**Table 3.** Kinetics of SSP of DBEDOT, as Determined by Different Methods

$T/^\circ\text{C}$	gravimetry: $t_{1/2}/\text{min}$	DSC: $t_{1/2}/\text{min}$	ESR: $t_{\max}/\text{min}$
60			470
65	200	228	270
70	105	135	148
75		88	83
80	45	46	53
85		27	
90		14	
$E_a/\text{kcal/mol}$	$23.2 \pm 2.3$	$27.1 \pm 1.1$	$25.9 \pm 0.6$
$\ln A$	$-29.3 \pm 3.4$	$-34.9 \pm 1.5$	$-33.0 \pm 0.8$
$R$	0.995	0.997	0.999
$s_0$	0.107	0.092	0.038

50% of the heat, which in most cases (except the fastest reaction at 90 °C) is close to the  $w_{\max}$ . The position of the exothermic peaks depends on the reaction temperature, and plotting  $\ln(1/t_{1/2})$  vs  $1/T$  according to the Arrhenius equation gives an activation energy of  $27.1 \pm 1.1$  kcal/mol with a high correlation coefficient (Figure 10, Table 3):

$$\ln k = \ln(1/t_{1/2}) = \ln A - E_a/RT$$

Extrapolation of the Arrhenius plot to 20 °C predicts the half-life time of DBEDOT around 70 days, which qualitatively fits the observation of decomposition of the material at room temperature.

**Gravimetric Analysis.** The solubility of DBEDOT in organic solvents decreases drastically during the polymerization due to (a) increased molecular weight and (b) formation of bromine salts from higher oligomers. Therefore, the conversion can be

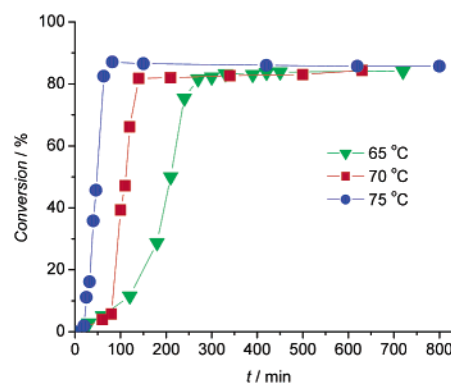


**Figure 11.** Conversion percentage vs reaction time of thermal polymerization of DBEDOT at different temperatures.

quantitatively followed by extraction of the crude reaction product (with  $\text{CHCl}_3$ ) and gravimetric analysis of the residue.<sup>7b,22</sup> The resulting kinetic curves, measured at different temperatures, are presented in Figure 11. As in the DSC experiments, the initial period is characterized by a low increase in conversion (induction period), which might be associated with an auto-catalytic effect of bromine and also strain energy accumulated during the reaction.<sup>23</sup> The difference between the final weight ( $\sim 85\%$ ) and the theoretical 100% value is due to release of molecular bromine (according to elemental analysis, the doping level in the final product, before vacuum drying, is 1.4 bromine atoms per EDOT unit, which corresponds to 16% of the weight loss). The observed “final conversion” in these experiments only indicates complete transformation of all starting DBEDOT, although further polymerization of higher oligomers may still take place. However, the mass spectral analysis of the extracts showed no dimer present in the reaction mixture in detectable quantities at any time, which is consistent with a chain reaction mechanism including formation of reaction centers and relatively fast polymer chain growth. An activation energy was found from the Arrhenius equation to be  $23.2 \pm 2.3$  kcal/mol (Figure 10, Table 3), which is somewhat lower than that found in the DSC analysis but also is less reliable because it is based on only three points.

**ESR Analysis.** Since the reaction in question produced an ESR active, doped polymer from the ESR silent monomer (DBEDOT), it could be followed by in situ ESR experiments (see SI). Again, there is a temperature-dependent induction period before the ESR signal intensity starts to increase rapidly, indicating formation of radical intermediates (Figure 12). While the polymerization proceeds, consumption of the monomer prevents creation of new radical species; therefore, the ESR intensity reaches a maximum and then decreases to a steady value, corresponding to radical concentration in the doped SSP-PEDOT. This is in agreement with the fact that the time to reach a maximum in the ESR intensity ( $t_{\max}$ ) is equal (or somewhat higher) than the reaction half-time, determined by DSC or gravimetry. The higher the heating temperature, the shorter the time needed to reach a maximum ESR signal. The ratio of the signal intensity in the maximum to that at the final conversion also changes with temperature from 3.5 at higher temperatures to 1.5 at lower temperatures (Figure 12). This can be interpreted as increasing concentration of radical intermediates formed at higher temperatures.

(23) Chance, R. R.; Sowa, J. M. *J. Am. Chem. Soc.* **1977**, *99*, 6703.

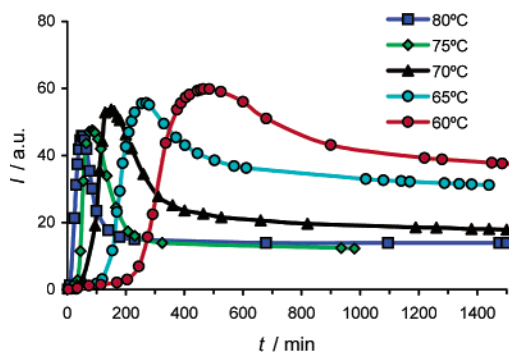


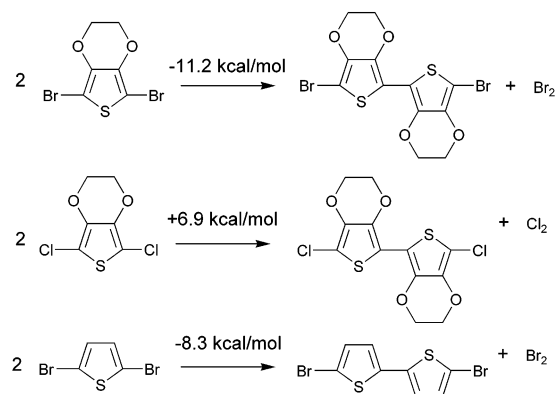
**Figure 12.** ESR kinetic curves of the polymerization of DBEDOT at 60–80 °C.

Plotting the  $t_{\max}$  versus temperature in  $\ln(1/t) - 1/T$  coordinates (according to the Arrhenius equation) gives a straight line with excellent correlation parameters (Figure 10). Assuming (with certain approximation) that the time of the maximum radical concentration is inversely proportional to the constant rate ( $k \approx 1/t_{\max}$ ), the above dependence can be used to acquire the activation energy of this solid-state polymerization (Table 3):  $E_a = 25.9 \pm 0.6$  kcal/mol, which is very close to the values determined in the DSC and gravimetric experiments.

**The Influence of Substituents and “Leaving Group”.** To better understand the reaction, it was important to compare the reactivity of different substituted dihalothiophenes, although we were limited by a low melting point for a number of derivatives (e.g., 2,5-dibromothiophene). Studying the reactivity in the three dihalosubstituted EDOTs revealed that, surprisingly, DBEDOT is not only much more reactive than DCEDOT, which does not polymerize at all below 60 °C (melting point), but also more reactive than DIEDOT. In the DSC, the  $t_{1/2}$  of polymerization of DIEDOT is 30 min at 160 °C (cf. DBEDOT parameters in Table 3). Accordingly, in bulk synthesis, a reaction time of 2–3 days is required to complete the polymerization of DIEDOT at 140 °C, which also affords highly conductive SSP-PEDOT ( $^{13}\text{C}$  NMR and elemental analysis confirms the structure of the product, see Table 1, sample PEDOT-E, and SI). The electron-donor 3,4-ethylenedioxy substituent also plays an important role in this SSP. Its replacement with electron-acceptor bromine atoms completely suppresses the polymerization: no sign of decomposition of tetrabromothiophene was found after incubating this compound at 115 °C for 2 weeks. We believe that the low oxidation potential of the thiophene monomer as well as high reduction potential of the halogen dopant are the key factors in this reaction, and the doping of the intermediate oligomers with molecular halogen (formed from the Br/I leaving groups) provides a driving force for the polymer growth. Exposing DBEDOT crystals to molecular bromine at room-temperature results in fast polymerization observed on the crystal surface.<sup>24</sup> In support of this hypothesis, the observed low reactivity of DIEDOT can be explained by the lower oxidation potential of iodine, which cannot dope small oligomers.

To summarize, although the complexity of this multistage solid-state reaction does not allow a simple kinetic analysis of the reaction, it is remarkable that three independent kinetic experiments give similar activation energy,  $E_a \approx 26$  kcal/mol. This activation energy (associated with the initiation event in

**Scheme 2.** Calculated Energies for Dimerization of Dihalosubstituted Thiophenes



the crystal) is quite close to the value found for SSP of diacetylene (22 kcal/mol),<sup>22</sup> although the reaction enthalpy ( $\Delta H_p \approx -14$  kcal/mol) is substantially lower than that of diacetylene polymerization ( $-36$  kcal/mol). The ESR monitoring strongly suggests radical (or radical ion) species as the reaction intermediates.

**Calculation of the Energies of Elementary Reactions Involved in the Polymerization.** To assess the possible polymerization mechanism we performed quantum mechanical density functional calculations at the B3LYP/6-31G(d) level<sup>25</sup> (including unscaled zero-point vibrational energies).<sup>26,27</sup> The following model reactions were studied (Scheme 2).

The analysis of the results allows to draw the following conclusion: Dimerization of DBEDOT is exothermic by 11.2 kcal/mol ( $\Delta G = 9.4$  kcal/mol), similar to dimerization of 2,5-dibromothiophene (exothermic by 8.3 kcal/mol). Dimerization of DCEDOT is endothermic by 6.0 kcal/mol. Polymerization to produce PEDOT from DBEDOT is also expected to be exothermic by roughly 10 kcal/mol, in good agreement with DSC measurements ( $\sim 14$  kcal/mol), taking into account enthalpy of in situ doping with bromine. We note that our calculations neglect steric effects in polymer formation which are expected to be relatively small due to the possibility of anti conformation of thiophene rings.<sup>28</sup>

The reaction mechanism remains speculative. A neutral radical polymerization is not expected to proceed at 60 °C in the dark, since the calculated homolytic cleavage of a C–Br bond in DBEDOT requires 85.0 kcal/mol, similar to homolytic cleavage of a C–Br bond in the nonpolymerizable dibromothiophene (84.3 kcal/mol). This is even higher than in bromoform,  $\text{expt } 72.1 \pm 0.3$  kcal/mol,<sup>29</sup> indicating a very strong

(25) (a) Lee, C.; Yang W.; Parr, R. G. *Phys. Rev. B* **1988**, *37*, 785. (b) Becke, A. D. *J. Chem. Phys.* **1993**, *98*, 5648.

(26) All calculations used the GAUSSIAN 98 series of programs. Frisch, M. J.; Trucks, G. W.; Schlegel, H. B.; Scuseria, G. E.; Robb, M. A.; Cheeseman, J. R.; Zakrzewski, V. G.; Montgomery, Jr., J. A.; Stratmann, R. E.; Burant, J. C.; Dapprich, S.; Millam, J. M.; Daniels, A. D.; Kudin, K. N.; Strain, M. C.; Farkas, O.; Tomasi, J.; Barone, V.; Cossi, M.; Cammi, R.; Mennucci, B.; Pomelli, C.; Adamo, C.; Clifford, S.; Ochterski, J.; Petersson, G. A.; Ayala, P. Y.; Cui, Q.; Morokuma, K.; Rega, N.; Salvador, P.; Dannenberg, J. J.; Malick, D. K.; Rabuck, A. D.; Raghavachari, K.; Foresman, J. B.; Cioslowski, J.; Ortiz, J. V.; Baboul, A. G.; Stefanov, B. B.; Liu, G.; Liashenko, A.; Piskorz, P.; Komaromi, I.; Gomperts, R.; Martin, R. L.; Fox, D. J.; Keith, T.; Al-Laham, M. A.; Peng, C. Y.; Nanayakkara, A.; Challacombe, M.; Gill, P. M. W.; Johnson, B.; Chen, W.; Wong, M. W.; Andres, J. L.; Gonzalez, C.; Head-Gordon, M.; Replogle, E. S.; Pople, J. A. *Gaussian 98*, Revision A.11.4; Gaussian, Inc.: Pittsburgh, PA, 2002.

(27) All optimized structures were found to be minima by frequency analysis.

(28) In addition, our calculations show that the “dimer” of DBEDOT has coplanar thiophene rings, in contrast to dibromobisthiophene, which has a twist angle of 21°.

(24) We note however, that a trace amount of HBr cannot initiate the SS polymerization of DBEDOT at room temperature, ruling out the possible acid catalysis of the polymerization.



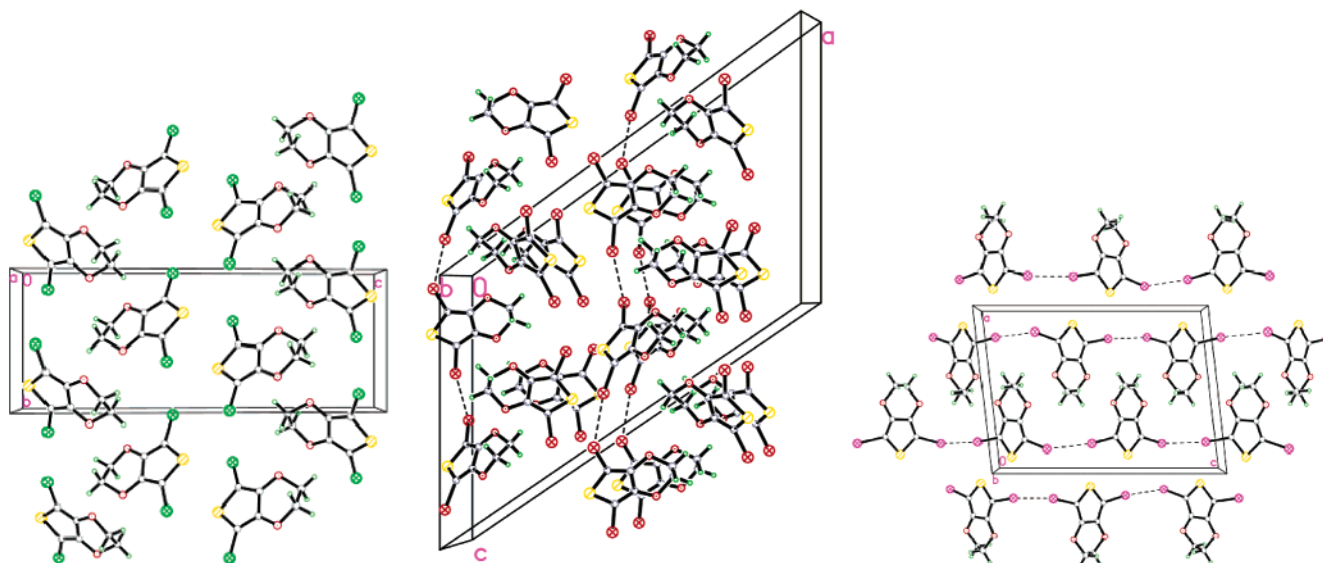
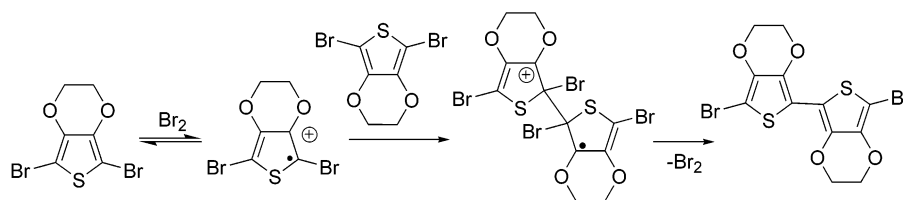


**Figure 13.** Crystal packing diagram of **DCEDOT** (left), **DBEDOT** (middle), and **DIEDOT** (right): (red ⊗) bromine atoms; (○) carbon atoms; (green ⊗) chlorine atoms; (green ○) hydrogen atoms; (magenta ⊗) iodine atoms; (yellow ○) sulfur atoms; (- - -) short intermolecular contacts between halogen atoms.

**Scheme 3.** Proposed Mechanism of the Initiation of SSP of DBEDOT



C–Br bond in DBEDOT. The most notable difference between DBEDOT and dibromothiophene, due to the electron-donating ethylenedioxy substituent in the former, is the stability of the cations produced by hererolytic cleavage of a C–Br bond to a carbocation and  $\text{Br}^-$ . Dissociation of dibromothiophene to produce bromothiophene cation requires, *in the gas phase*, 221.1 kcal/mol, while dissociation of DBEDOT to produce mono-bromo-EDOT cation requires 201.3 kcal/mol.

On the basis of the above studies we propose an oxidative polymerization mechanism for DBEDOT, similar to oxidation of thiophenes by  $\text{FeCl}_3$  (the reduction potential of  $\text{Br}_2$  [1.07 V] is 0.3 V higher than that of  $\text{FeCl}_3$  [0.77 V], in solution; in the solid the difference is unknown). The reaction is autocatalytic, catalyzed by the released bromine (Scheme 3).

**Crystallographic X-ray Analysis of Dihalogen-EDOTs.** To understand the importance of the crystal structure on this polymerization reaction, single crystals of three dihalogen-substituted EDOTs (dichloro-, dibromo-, and diiodo-) were grown from EtOH solution and studied by X-ray analysis (Figure 13). The molecular units do not have any particular feature which could explain the solid-state reactivity: C–Hal distances (1.705 Å for C–Cl, 1.87 Å for C–Br, 2.08 Å for C–I) are usual for normal C–Hal single bonds. In all three compounds, the thiophene molecules form stacks whose axes are significantly tilted from the normal ( $40\text{--}45^\circ$ ).<sup>30</sup> This tilt results in a considerable shift of the adjacent molecules and precludes  $\pi\text{--}\pi$  interaction within the stacks, despite a favorable interplanar distance of 3.5 Å. The interaction within the stack occurs via

halogen atoms positioned over the aromatic ring of an adjacent molecule. In all three structures, the stacks form rows, running along the crystallographic *b* axis (for DCEDOT) and *c* axis (for DBEDOT and DIEDOT). The sulfur atoms are situated on the same side of a row, but in adjacent rows the sulfurs are opposed. Hydrogen bonds between ethylenedioxy fragments of different rows provide a dimerized row architecture; there are also weak  $\text{S}\cdots\text{S}$  contacts between the molecules of adjacent row dimers in DBEDOT and DIEDOT.<sup>31</sup> In DCEDOT the thiophene molecules of stacks within the same row (and adjacent row of another dimer) are parallel, forming a quasi-sheet structure (i.e. a continuous two-molecule-wide lane). The closest  $\text{Cl}\cdots\text{Cl}$  contact (3.58 Å) is found between molecules in the same row, but the distance is longer than the sum of van der Waals (vdW) radii (3.5 Å). The “superstack” architecture in DIEDOT is somewhat similar, but the above quasi-sheets direction is perpendicular to the row. In DBEDOT the planes of molecules in *all* adjacent stacks are significantly tilted relative to each other, so that the only parallel adjacent DBEDOT molecules are found within the stack. An important packing feature of DBEDOT and DIEDOT, possibly governing their reactivity in the solid state, is a remarkably short intermolecular  $\text{Hal}\cdots\text{Hal}$  contact: 3.45 and 3.50 Å for DBEDOT<sup>32</sup> and 3.73 Å for DIEDOT [cf. the sum of vdW radii is 3.7 Å ( $\text{Br}\cdots\text{Br}$ ) and 4.0 Å ( $\text{I}\cdots\text{I}$ )]. These contacts occur between almost perpendicular

(31) DBEDOT: shortest  $\text{S}\cdots\text{S}$  is 3.56 Å (double vdW radius 3.6 Å),  $\text{S}\cdots\text{Br}$  is 3.62 Å (sum of vdW radii 3.65 Å),  $\text{O}\cdots\text{H}$  are 2.47, 2.62, and 2.69 Å (sum of vdW radii 2.9 Å). DIEDOT shortest  $\text{S}\cdots\text{S}$  is 3.49 Å (double vdW radius 3.6 Å),  $\text{S}\cdots\text{I}$  is 3.81 Å (sum of vdW radii 3.86 Å),  $\text{O}\cdots\text{H}$  are 2.46 and 2.60 Å.

(32) This structure consists of two nonequivalent DBEDOT molecules, belonging to different rows.

(29) Blanksby, S. J.; Ellison, G. B. *Acc. Chem. Res.* **2003**, *36*, 255.

(30) The stack axis is parallel to the crystallographic *b* axis for DBEDOT and DIEDOT, and to the *a* axis for DCEDOT.

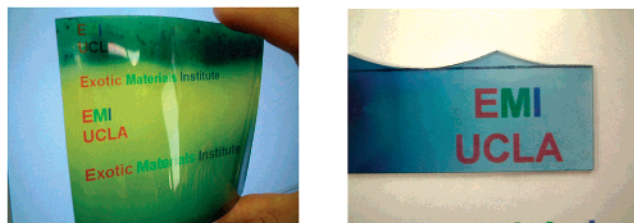


**Figure 14.** Semitransparent conducting films of PEDOT on a plastic substrate (left) and a glass slide (right), prepared by in situ SSP of vacuum deposited DBEDOT.

molecules, so that the angle C–Hal···Hal is 106.7° (DBEDOT) and 101.6° (DIEDOT), in contrast to a 180° geometry of these contacts in DCEDOT.

The most probable direction of polymerization would be formation of a C–C bond between C-2 and C-5 atoms of the adjacent thiophene molecules of the same stack, facilitated by Hal···Hal interaction between the molecules of adjacent stacks in the same row. The corresponded intermolecular C···C distance is 3.78 Å for DIEDOT, 4.09 Å for DBEDOT and 4.27 Å for DCEDOT. The observed SSP, however, requires significant rotation of the molecules (see SI).

In summary, the specific stacking structure of DBEDOT and DIEDOT and, especially, close Hal···Hal contacts obviously play an essential role in the SSP of these compounds. However, we could not find a crystal motif that would allow a, difficult to imagine, topotactic polymerization (due to the required expulsion of excess halogen). Most likely, the polymerization occurs along the stacks of the monomer, but must be accompanied by significant rotation and some movement of the molecules.

**Applications in Plastic Electronics.** We believe that the described polymerization of DBEDOT that occurs under very gentle conditions and does not require external agents will have many practical applications; as, for example, all-organic light-emitting diodes, polymer field-effect transistors, etc. By virtue of a simple fabrication procedure and higher degree of order, SSP-PEDOT constitutes an efficient alternative to the water-processable Baytron PEDOT material, which affords films with surface resistance as high as  $10^5 \Omega/\square$ .<sup>4</sup> The time instability problem, usually associated with halogen-doped conducting polymers, seems not to be an issue for our SSP-PEDOT, as demonstrated by the highest conductivity of the 2-year-old sample.

Here we demonstrated a facile preparation of highly conductive polymer films on an insulating support as an important step to creating all-organic electronics. A reduced pressure ( $\sim 10$  mbar) sublimation of DBEDOT, with gentle heating of the substrate, results in in situ deposition onto glass slides (or a plastic substrate, Figure 14) of semitransparent blue uniform PEDOT films.<sup>33</sup> The average surface resistances of the glass slide and the plastic substrate are  $2.1 \times 10^3 \Omega/\square$  and  $3.6 \times 10^3 \Omega/\square$ , respectively, at an average thickness of 2700 and 1300 Å, respectively. The surface conductivity reaches 20 S/cm. Further doping with iodine vapor increases the conductivity of the films by a factor of 2–3. The very high surface conductivity of the present thin films is comparable and even higher than

that of recently reported PEDOT–glycerol and PEDOT–sorbitol composite films used in creation of all-organic photovoltaic cells (surface resistance:  $\sim 10^3 \Omega/\square$ , conductivity:  $\sim 10$  S/cm).<sup>4</sup>

## Conclusions

We have shown that heating of dibromo- and diiodo-3,4-ethylenedioxythiophene in the solid state results in an unprecedented coupling self-reaction and gives highly conducting and relatively well-ordered halogen-doped poly-3,4-ethylenedioxythiophene. X-ray analysis of the monomers indicates very close Hal···Hal contacts, which facilitate this unusual reaction in the solid state. The solid-state polymerization of DBEDOT is exothermic by 14 kcal/mol and requires an activation energy of  $\sim 26$  kcal/mol. ESR monitoring of the reaction indicates that a radical (or an ion-radical) polymerization mechanism and kinetic behavior are similar to those observed in SSP of diacetylene. Polymerization of DBEDOT above the melting point leads to a lower-conductivity polymer. The temperature dependence of the conductivity of SSP-PEDOT reveals a semiconducting behavior. Highly conducting thin films of PEDOT can be easily fabricated using our method.

This work marks the first synthesis of conducting polythiophenes in the solid state. The strategy will be applied to other conducting polymer systems through a rational design of the monomers and should have a substantial technological impact.

## Experimental Section

**Materials.** Reagent chemicals were purchased either from Aldrich or Fisher Chemical Co. 3,4-Ethylenedioxythiophene (EDOT) was kindly donated by Bayer Co. and was distilled (120–122 °C/10 mmHg) before use. Chloroform and acetonitrile were distilled from calcium hydride under an argon atmosphere. Other solvents and reagents were used as received.

**Measurements.** Solution NMR spectra were taken on a Bruker ARX 500 spectrometer. All chemical shifts ( $\delta$ ) are reported relative to tetramethylsilane (TMS) at 0.0 ppm. The solid state <sup>13</sup>C NMR spectra were acquired on a Bruker Avance 300 spectrometer operating at 75.476 MHz. The samples were ground and packed into zirconium oxide rotors with Kel-F end caps for use in a 4-mm magic angle spinning probe from Bruker. The data were acquired at spinning rate of 10 kHz with variable amplitude cross-polarization experiments.<sup>34</sup> The <sup>13</sup>C NMR chemical shifts were referenced to an external sample of adamantane with the methylene resonance assigned to 38.03 ppm. As a secondary reference for a <sup>13</sup>C scale, tetramethylsilane was assigned 0.0 ppm.

The EPR measurements were performed with a Bruker EMX X-band spectrometer at 9.78 GHz, using a microwave bridge and a rectangular TE102 cavity. The temperature of the samples was controlled between 90 and 400 K by a flow of either cooled or heated nitrogen gas, and between 4 and 300 K by a flow of helium gas. The modulation frequency was 100 kHz, and the modulation amplitude used 0.1–4 Hz. For the temperature-dependent ESR experiments, a single “crystal” (3 mg) of SSP-PEDOT was sealed in a quartz ESR tube in a vacuum and cooled to the lowest achievable temperature (4–5 K). The data were acquired after gradual warming up to the higher temperatures and stabilizing for 20 min before recording the spectrum.

X-ray crystallographic data were collected on a Bruker Smart 1K X-ray diffractometer equipped with a large area CCD detector. Single crystals of each compound were mounted on a glass fiber, and

(33) The greenish shading of the flexible substrate in Figure 14 is due to bromination of the upper layer of commercial ink-jet transparency used in this experiment with excess of bromine (gives yellow color).

(34) Peersen, O. B.; Wu, X.; Kustanovich, I.; Smith, S. O. *J. Magn. Reson., Ser. A* **1993**, *104*, 334.

diffraction data were acquired using a Mo K $\alpha$  radiation source ( $\lambda = 0.71073 \text{ \AA}$ ) at 100 K. Structure solution and refinement were conducted using a SHELXTL package from Bruker (see SI for details).

The powder and thin film X-ray diffraction experiments were performed on Bruker AXS D8 Advance X-ray diffractometer, with Cu K $\alpha$  radiation source ( $\lambda = 1.5406 \text{ \AA}$ ) in  $\Theta/2\Theta$  mode, at room temperature.

FT-IR spectra were recorded on a Perkin-Elmer 1 spectrometer in KBr pellets. UV–visible spectra were obtained on a Shimadzu UV–NIR 3100 spectrophotometer. Melting points were measured using a capillary melting point apparatus (MelTemp from Laboratory Devices) and are uncorrected. Thermogravimetric analysis (TGA) was carried out on a Perkin-Elmer TAC 7/DX Thermal Analyst system at a heating rate of  $10 \text{ }^\circ\text{C}/\text{min}$  and at a nitrogen flow rate of  $75 \text{ cm}^3/\text{min}$ . Differential scanning calorimetry (DSC) was run on a Perkin-Elmer DSC Pyris instrument.

Cyclic voltammetry (CV) was performed on a BAS 100B Electrochemical Analyzer with a three-electrode cell in a MeCN solution of  $0.1 \text{ M Bu}_4\text{NPF}_6$  at a scan rate of  $50 \text{ mV/s}$ . The polymer films were in situ sublimed on a platinum electrode ( $0.5 \text{ cm}^2$ ) by heating the monomer DBEDOT crystals at  $60 \text{ }^\circ\text{C}$  in a vacuum overnight (the sublimator was evacuated to  $10 \text{ mbar}$ , closed, and incubated at  $60 \text{ }^\circ\text{C}$  for  $24 \text{ h}$ ). A Pt wire was used as the counter electrode and an  $\text{Ag}/\text{Ag}^+$  ( $0.01 \text{ M}$  of  $\text{AgNO}_3$  and  $0.1 \text{ M}$  of  $\text{Bu}_4\text{NPF}_6$  in MeCN) electrode was used as the reference electrode. Its potential was corrected by measuring the ferrocene/ferrocenium couple in this system ( $0.11 \text{ V}$  versus  $\text{Ag}/\text{Ag}^+$ ).

Elemental analyses were performed by Desert Analytics Co.

**2,5-Dibromo-3,4-ethylenedioxythiophene (DBEDOT).**<sup>5c,12</sup> To a stirred solution of 3,4-ethylenedioxythiophene (EDOT) ( $14.0 \text{ g}$ ,  $0.10 \text{ mol}$ ) dissolved in a 2:1 solvent mixture of chloroform ( $300 \text{ mL}$ ) and acetic acid ( $150 \text{ mL}$ ) was added slowly *N*-bromosuccinimide ( $36.0 \text{ g}$ ,  $0.202 \text{ mol}$ ) at  $0\text{--}5 \text{ }^\circ\text{C}$  under argon atmosphere. The mixture was allowed to stir for  $8 \text{ h}$  at room temperature and quenched with water. The organic layer was separated, and the water layer was extracted with chloroform ( $100 \text{ mL} \times 3$ ). The combined chloroform extract was neutralized with 5% sodium bicarbonate solution, washed with distilled water, and dried with anhydrous magnesium sulfate. The filtered solution was concentrated, passed through a silica gel column, and eluted with methylene chloride to give a crude white powder. It was recrystallized from ethanol to produce  $22.8 \text{ g}$  of white needlelike crystals in 76% yield, mp  $96\text{--}97 \text{ }^\circ\text{C}$ . MS  $m/z$ : 298, 300, 302 ( $\text{M}^+$ , 55, 100, 55).  $^1\text{H NMR}$  ( $500 \text{ Hz}$ ) ( $\text{CDCl}_3$ ),  $\delta_{\text{H}}$  4.27 (s, 4 H) ppm.  $^{13}\text{C NMR}$  ( $125 \text{ Hz}$ ) ( $\text{CDCl}_3$ ),  $\delta_{\text{C}}$  139.6, 85.4, 64.9. CP-MAS  $^{13}\text{C NMR}$  ( $75 \text{ Hz}$ , solid state),  $\delta_{\text{C}}$  140.3, 84.6, 65.1. Elemental analysis: Found: C, 23.79; H, 1.28; Br, 53.00; S, 10.86; Calculated for  $\text{C}_6\text{H}_4\text{Br}_2\text{O}_2\text{S}$ , C, 24.02; H, 1.34; Br, 53.27; S, 10.69.

**2,5-Dichloro-3,4-ethylenedioxythiophene (DCEDOT)**<sup>5d</sup> was obtained by a method similar to that for DBEDOT, using *N*-chlorosuccinimide NCS instead: white needles (80%), mp  $60\text{--}62 \text{ }^\circ\text{C}$ . MS (EI):  $m/z$  209.9 (100%). HRMS (EI): 209.93054; calcd For  $\text{C}_6\text{H}_4\text{Cl}_2\text{O}_2\text{S}$ : 209.93091.  $^1\text{H NMR}$  ( $500 \text{ MHz}$ ;  $\text{CDCl}_3$ ): 4.25.  $^{13}\text{C NMR}$  ( $125 \text{ MHz}$ ;  $\text{CDCl}_3$ ): 137.2, 100.3, 64.8. El. Anal. Found: C, 34.15; H, 1.85; Cl, 33.24; S, 15.27. Calcd for  $\text{C}_6\text{H}_4\text{Br}_2\text{O}_2\text{S}$ : C, 34.14; H, 1.91; Cl, 33.59, S, 15.19.

**2,5-Diiodo-3,4-ethylenedioxythiophene (DIEDOT).** Method 1. To a solution of EDOT ( $5.84 \text{ g}$ ,  $0.041 \text{ mol}$ ) in anhydrous THF at  $-78 \text{ }^\circ\text{C}$  was added *n*-BuLi ( $2.5 \text{ M}$  in hexane;  $40 \text{ mL}$ ,  $0.10 \text{ mol}$ ) in THF ( $10 \text{ mL}$ ). The reaction mixture was allowed to warm to  $0 \text{ }^\circ\text{C}$  for  $30 \text{ min}$  and cooled to  $-78 \text{ }^\circ\text{C}$ , and iodine crystals ( $13 \text{ g}$ ,  $0.051 \text{ mol}$ ) were added in one portion. The reaction mixture was allowed to warm to  $20 \text{ }^\circ\text{C}$  overnight, the solvent was removed in vacuo, and the residue was taken up in  $\text{CHCl}_3$ . After washing with KI solution (to remove excess iodine) and water, the organic layer was concentrated in vacuo and purified by flash chromatography on silica eluting with benzene/chloroform (2:1 v/v), followed by recrystallization from EtOH to give pure DIEDOT as yellow crystals ( $6.91 \text{ g}$ , 43%), mp  $185\text{--}188 \text{ }^\circ\text{C}$  dec. MS (EI):  $m/z$

$393.8$  (100%,  $\text{M}^+$ ). HRMS (EI): 393.80233; calcd For  $\text{C}_6\text{H}_4\text{I}_2\text{O}_2\text{S}$ : 393.80216.  $^1\text{H NMR}$  ( $500 \text{ MHz}$ ;  $\text{CDCl}_3$ ): 4.26.  $^{13}\text{C NMR}$  ( $125 \text{ MHz}$ ;  $\text{CDCl}_3$ ): 143.7, 65.0, 51.7. Elemental analysis found: C, 18.46; H, 0.84; S, 7.93; calculated for  $\text{C}_6\text{H}_4\text{O}_2\text{SI}_2$ : C, 18.29; H, 1.02; S, 8.14.

**Method 2.** To a mechanically stirred solution of EDOT ( $1.40 \text{ g}$ ,  $0.01 \text{ mol}$ ) in acetic acid ( $100 \text{ mL}$ ) was added dropwise of a solution of mercuric acetate ( $6.40 \text{ g}$ ,  $0.02 \text{ mol}$ ) in acetic acid ( $200 \text{ mL}$ ) over  $2 \text{ h}$ . A white precipitate formed, and the reaction mixture was stirred overnight. The white precipitate was filtered, washed with methanol and diethyl ether, and dried under vacuum to give a white product of 2,5-diacetoxymercuri-EDOT ( $6.25 \text{ g}$ , yield 95%). This compound is insoluble in common organic solvents, mp  $> 350 \text{ }^\circ\text{C}$ . MS (EI)  $m/z$  659 (100%,  $\text{M}^+$ ). Elemental analysis found: C, 18.18; H, 1.51; Hg, 61.03; S, 4.81 calculated for  $\text{C}_{10}\text{H}_{10}\text{Hg}_2\text{O}_6\text{S}$ , C, 18.21; H, 1.53; Hg, 60.84; S, 4.86.

To a mechanically stirred suspension of the above white powder ( $5.00 \text{ g}$ ,  $0.0075 \text{ mol}$ ) in acetonitrile ( $500 \text{ mL}$ ) was added dropwise a solution of iodine ( $4.06 \text{ g}$ ,  $0.016 \text{ mol}$ ) in acetonitrile ( $300 \text{ mL}$ ). During the addition of iodine, the suspension cleared to produce a yellow solution. After evaporation of the solvent, the residue was dissolved in a saturated potassium iodide aqueous solution. The product was extracted with chloroform ( $50 \text{ mL} \times 3$ ) from the aqueous solution. After evaporation of the solvent, the crude product was recrystallized from ethanol to produce light brown crystals ( $1.63 \text{ g}$ , yield 55%), mp  $189 \text{ }^\circ\text{C}$ . Spectral data were identical to the sample obtained in method 1.

**SSP-PEDOT.** In a typical experiment DBEDOT ( $0.01\text{--}2 \text{ g}$ ) was incubated at  $60 \text{ }^\circ\text{C}$  for  $24 \text{ h}$  in a closed vial, during which period the color of the material changed from white to black and a brown bromine vapor appeared in the vial. Performing the reaction in an inert atmosphere (Ar) or in a vacuum-sealed vial does not have any apparent effect on the polymerization time or the properties of the product. El. Anal. Found: C, 27.56; H, 1.53; Br, 41.77; S, 12.19. Calcd for  $\text{C}_6\text{H}_4\text{-Br}_{1.4}\text{O}_2\text{S}(\text{H}_2\text{O})_{0.6}$ : C, 27.41; H, 1.98; Br, 42.56; S, 12.20. The polymer was vacuum-dried overnight to afford the bromine-doped polymer (PEDOT-A in Table 1). El. Anal. Found: C, 28.87; H, 1.65; Br, 38.42; S, 12.90. Calcd for  $\text{C}_6\text{H}_4\text{Br}_{1.2}\text{O}_2\text{S}(\text{H}_2\text{O})_{0.6}$ : C, 29.19; H, 2.10; Br, 38.84; S, 12.99.

The well-ground material was additionally dried in a vacuum ( $0.1 \text{ mbar}$ ) at  $150 \text{ }^\circ\text{C}$  overnight, then dispersed in MeCN ( $200 \text{ mL/g}$ ) and stirred with 50% hydrazine hydrate ( $10 \text{ mL/g}$ ) overnight, filtered, and washed with neat MeCN. Vacuum drying afforded a nearly fully dedoped PEDOT-C (see Table 1). El. Anal. Found: C, 46.84; H, 2.42; Br, 0.42; S, 19.04. Calcd for  $\text{C}_6\text{H}_4\text{O}_2\text{Br}_{0.01}\text{S}(\text{NH}_2\text{NH}_2 \cdot 3\text{H}_2\text{O})_{0.12}$ : C, 47.63; H, 3.44; N, 2.22; Br, 0.53; S, 21.19. CP-MAS  $^{13}\text{C NMR}$  ( $75 \text{ MHz}$ , solid state):  $\delta_{\text{C}}$  136.5, 108.7, 64.9; IR (KBr):  $\nu = 1645, 1510, 1431, 1357, 1202, 1069, 984, 920, 849$ .

**SSP-PEDOT Films on Different Substrates.** A crystalline DBEDOT sample ( $\sim 100 \text{ mg}$ ) was placed in a  $200\text{-mL}$  sublimation apparatus together with substrates of interest (microscope slides, plastic films, platinum sheets). The system was evacuated to ca.  $10 \text{ mbar}$ , sealed, and incubated in an oven at  $60 \text{ }^\circ\text{C}$  for  $24 \text{ h}$  to produce a blue film on the inside surface of the apparatus and the above substrates. The correct pressure should be kept to get uniform good quality films (mind the increase of the actual pressure in the system due to bromine liberation).

**Acknowledgment.** We thank the United States Air Force Office of Scientific Research for support through F49620-00-1-0103, the Army Research Office for support of a MURI through DAAD19-99-1-0316, and the National Computational Science Alliance for support under DMR020033N. D.F.P. acknowledges the support from the Natural Sciences and Engineering Research Council of Canada for support through a Discovery Grant. We thank Dr. R. Helgeson at EMI, UCLA, and Dr. Z. Bao, Lucent Technologies, for many valuable discussions. We are grateful to Mr. J. Huang for TEM measurements, Dr. S. I. Khan for X-ray crystallographic



analysis, Dr. R. E. Taylor and Dr. J. Strouse for help with solid-state  $^{13}\text{C}$  NMR and cryostatic ESR measurements (Department of Chemistry and Biochemistry, UCLA).

**Supporting Information Available:** Plot of the ESR line width vs temperature; ESR spectrum of the dedoped SSP-PEDOT; 2D graph of evolution of the ESR signal during the polymerization; TGA analysis plot; details of the thermomicroscopy analysis and the recorded video files of the polymerization process (in avi format); cyclic voltammograms;

selected pictures of supramolecular architecture of DBEDOT, DCEDOT, and DIEDOT and the proposed scheme of SSP in DBEDOT; details of the X-ray crystallographic analysis and X-ray crystallographic files in CIF format for compounds DCEDOT, DBEDOT and DIEDOT. Absolute energies and optimized geometries (in Cartesian coordinates) for all calculated compounds at B3LYP/6-31G(d). This material is available free of charge via the Internet at <http://pubs.acs.org>.

JA037115Y